Available online at www.sciencedirect.com

SciVerse ScienceDirect

Procedia - Social and Behavioral Sciences 00 (2012) 000–000

Procedia Social and Behavioral Sciences

www.elsevier.com/locate/procedia

SIIV - 5th International Congress - Sustainability of Road Infrastructures

Impact of Connection between Specimen and Load Plate on Viscoelastic Material Response of Hot Mix Asphalt

Dr. Bernhard Hofko*, Prof. Ronald Blab

Vienna University of Technology, Research Center of Road Engineering, Gusshausstrasse 28/E 230/3, 1040 Vienna, Austria

Abstract

Cyclic compression tests (CCT) on hot mix asphalt (HMA) can be employed for determining the linear viscoelastic (LVE) material response. This paper investigates whether CCTs produce comparable results in terms of LVE material reaction. Test data evaluation is carried out by means of regression analysis with a standard sine and an advanced function containing the first harmonic oscillation term. From the findings it can be concluded that CCTs produce results that are comparable to results of the 4-point-bending (4PBB) tests. It is shown that the advanced regression analysis can be employed to analyze the response quality of the test machine.

Selection and/or peer-review under responsibility of SIIV2012 Scientific Committee

viscoelasticity; hot mix asphalt; stiffness testing; regression analysis; cyclic compression tests; four-point-bending test

1. Introduction

A comprehensive pioneering work in the field of triaxial cyclic compression tests (TCCT) on hot mix asphalt (HMA) started in the 1970s at the Belgian Road Research Center (BRRC). Having the main objective to develop a model to describe the permanent deformation behavior of HMA, TCCTs with varying test conditions were carried out to study the impact of different boundary conditions systematically. The derived BRRC-model by Francken (1977) [1] is still used for a first approximation of the permanent axial strain due to triaxial loading, and the test program was one major source for the development of the European standard for TCCT EN 12697-25 (2005) [2]. Jaeger (1980) [3] tested different HMAs at high temperatures with a sinusoidal axial compressive loading and constant radial confining pressure. It was shown that the magnitude of axial loading has the most significant impact on the permanent axial strain, followed by temperature and frequency of loading. This research was followed by Weiland (1986) [4]. Advanced technologies opened the possibility to digitalize the data, store,

* Corresponding author. Tel.: +0-000-000-0000 ; fax: +0-000-000-0000 .
E-mail address: author@institute.xxx

process and therefore evaluate and analyze test data in more detail. Amplitudes of stress and strain could be visualized and thus phase lags between those signals could be looked at for the first time. The results in [4] show that there is a difference between the phase angle of axial loading and axial deformation vs. axial loading and radial deformation. They also indicate that temperature has a dominant impact on the magnitude of the phase lag. In the 1990s von der Decken (1997) [5] presented an extensive study on TCCTs with cyclic confining pressure on different HMAs and at different temperatures. Interestingly enough, it was found that a constant phase lag between axial loading and radial deformation exists which is independent of mix design and temperature. It was set to 36°.

A recent, comprehensive study on the TCCT was carried out by Kappl (2007) [6]. The study contains an extensive testing program where a number of asphalt mixes with different aggregate and binder types were tested in the TCCT according to [2]. An attempt was made to link the results of TCCTs to various binder parameters or results of simple test methods like the Marshall test. The main findings are that there is a strong correlation between the softening point ring and ball and the cumulated, axial strain after 25,000 load cycles at 50°C. Also, the air void content could be linked to the creep rate resulting from the standard TCCT.

The TCCT was implemented into the series of harmonized European Standards for testing of HMA in 2004 as EN 12697-25 [2] to assess the resistance to permanent deformation at high temperatures. The standard test procedure consists of a cyclic dynamic axial loading to simulate a tire passing a pavement structure and a radial confining pressure to consider the confinement of the material within the pavement structure. The permanent axial strain is analyzed vs. the number of load cycles to obtain a creep curve.

However, cyclic compression tests (CCTs) can also be employed for assessing the material response (stiffness and phase lag) of HMA in the linear viscoelastic domain. In this case the test is run with frequency and temperature sweep [7]. Material parameters are obtained from the applied loading (action) and the reaction of the material (i.e. deformation) [8]. Different from tests with both tension and compression, e.g. the direction tension and compression test according to EN 12697-26 [9] where the specimens must be firmly connected to the load plates since tension is applied, two test setups are possible for CCTs: (a) Specimens can be glued and thus firmly connected to the load plates. This setup prevents transversal strain at and near the end planes of the specimen. A more homogeneous strain distribution can be achieved when (b) the specimen is placed in between the load plates without a firm connection. In this case friction-reducing additives (e.g. silicone grease) support transversal strain also at the end planes. This paper investigates whether the viscoelastic material response of HMA depends on the test setup, i.e. whether the specimen is firmly connected to the load plates or not. It also shows that an advanced function including the 1st harmonic oscillation term used for regression analysis of the test data can be employed to study distortion of the sinusoidal signal and thus reveal technical limits of the test machine and incorporated sensors.

2. Materials and Test Program

2.1. Materials and Specimen Preparation

For the presented research, an asphalt concrete with a maximum nominal aggregate size of 11 mm (AC 11) was used. The mix was composed of porphyry as the aggregate, powdered limestone as filler and an SBS-modified binder PmB 25/55-65. The main characteristics of the binder are listed in Table 1. The binder content was set to 5.3% (m/m) which is the optimal binder content according to Marshall. Fig. 1 shows the grading curve of the mix.

Table 1 Characteristics of PmB 25/55-65

Parameter	Value
Penetration at 25°C	46.0 $^{1}/_{10}$ mm
Softening Point Ring & Ball	73.0 °C
Performance Grade according to SHRP	>82-16

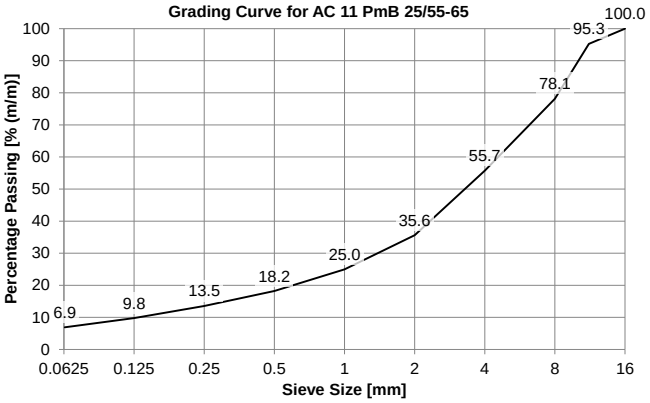

Fig. 1 Grading curve of the AC 11

The mix was produced in a reverse-rotation compulsory mixer. The pre-heated aggregates and filler were mixed for one minute before the pre-heated bitumen was added to the mix. Aggregates, filler and bitumen were mixed for an additional three minutes. The material was then compacted in a segment roller compactor to slabs with a base area of 500x260 mm and a target height of 130 mm. The slabs were produced in two layers, since single layer compaction leads to a larger scatter of density between upper and lower parts of the slab [10]. As stated in [10] the fact that the specimens incorporate an interface of two layers does not affect the test results compared to results from specimens taken from homogeneous slabs with single layer compaction.

From each slab, four specimens were cored out with a diameter of 100 mm. The obtained specimens were cut to a height of 200 mm. Fig. 2 shows a scheme of an HMA slab and the specimens obtained from the slab.

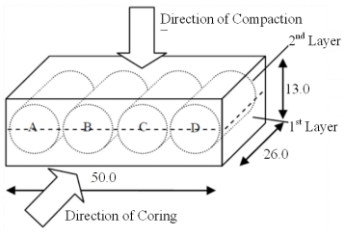

Fig. 2 Principle of specimen direction within HMA slab

2.2. Test Setup and Program

To investigate the impact of the connection between load plates and specimen on the viscoelastic material response, two different test setups were employed in the study. Fig. 3 shows a scheme of the two setups. The left setup (a) is a standard CCT without a firm connection between load plate and specimen. Silicone grease is applied to both end planes of the specimen to reduce friction and activate transversal strain at and near the end planes. In the right setup (b) the specimen is glued to both load plates with a two-component adhesive. Transversal strain is prevented in this test setup at the end planes of the specimen.

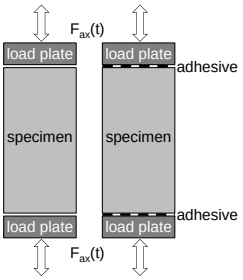

Fig. 3 Two test setups to compare results of mix-controlled and force-controlled CTTs

For each setup four specimens were tested. Details on the HMA specimens of the AC 11 mix are given in Table 2. In a detailed analysis preceding this study [7], CCTs were carried out on HMA specimens at different temperatures (10°C, 30°C, 50°C) and stress levels to isolate test conditions which stress specimens within the linear viscoelastic domain. According to Airey, et al. (2003) [11] a strain level of 10^{-4} or smaller ensures that HMA specimens are tested within the linear viscoelastic range. The results of the preceding analysis show that CCTs at 30°C, a mean axial stress of 0.25 N/mm² and a stress amplitude of 0.15 N/mm² keep the strain level below 10^{-4} and thus within the linear viscoelastic domain. A frequency sweep was carried out with frequencies ranging from 0.1 Hz to 10 Hz. Table 3 provides information on the number of load cycles carried out for each frequency.

Table 2 Specimen characteristics

Specimen Code	Air Void Content [% (v/v)]	glued/unglued
T404C	6.4	Unglued
T406E	5.5	
T406G	5.0	
T406H	7.0	
T404A	3.8	Glued
T405C	3.5	
T406A	5.2	
T406B	3.5	

Table 3 Number of load cycles for each frequency in the CCTs

Frequency	0.1	0.5	1.0	3.0	5.0	10.0
# of Load Cycles	20	50	100	100	200	200

Axial deformation was recorded by two LVDTs on top of the upper load plate. For data evaluation the mean value of the signals from both LVDTs was used. The radial deformation was obtained by strain gauges that were attached directly to the surface of the specimens. The strain gauges with an active length of 150 mm were located at half height along the circumference of the specimen.

To compare the material response from CCTs to a well-established, standardized stiffness test, four specimens of the same mix were tested in a 4-point-bending (4PBB) stiffness test according to [9]. The tests were run at 30°C with frequencies ranging from 0.1 Hz to 10 Hz. The strain amplitude for the tests was set to 35 µm/m. Details on the specimens can be found in Table 4.

Table 4 Specimen characteristics for 4PBB

Specimen Code	Air Void Content [% (v/v)]
E454A	4.3
E454B	4.6
E454D	3.9
E454F	4.0

3. Data Evaluation

Signal data from force and deformation sensors were investigated by means of regression analysis with two different functions:

$$f(t) = a_1 + a_2 \cdot \sin\left(2\pi \cdot f \cdot t + a_3\right) + a_4 \cdot t \quad (1)$$

$$f(t) = a_1 + a_2 \cdot \sin\left(2\pi \cdot f \cdot t + a_3\right) + a_4 \cdot t + a_5 \cdot \sin\left(4\pi \cdot f \cdot t + a_6\right) \quad (2)$$

where:

a_1 ..... *Offset of the fundamental oscillation*
a_2 ..... *Amplitude of the fundamental oscillation*
a_3 ..... *Phase lag of the fundamental oscillation*
a_4 ..... *Gradient of the linear tem*
a_5 ..... *Amplitude of the 1st harmonic oscillation*
a_6 ..... *Phase lag of the 1st harmonic oscillation*
f ..... *Frequency of the oscillation*
t ..... *Time*

The function according to equation (1) will be referred to as *F+L* for its two terms, the fundamental oscillation (*F*) and the linear term (*L*). The function according to equation (2) as *F+L+1H* for the additional 1st harmonic oscillation (*1H*). For data evaluation purposes the test data was divided into blocks of three load cycles. These blocks were used for the regression analysis. The reason for choosing three cycles per evaluation block is to achieve a stable regression analysis. The more complex *F+L+1H* regression was employed in this study because the parameters of the 1st harmonic can be used to analyze distortions of sinusoidal oscillation data by

mathematical means. As shown by Kappl (2007) [6] CCTs result in axial deformation of the specimen that cannot be described with a standard *F+L* regression according to equation (1). Fig. 4 shows a graphic example of the approximation of test data from a CCT with the *F+L* function. In the left diagram the test data of axial stress (σ_{ax}) and strain (ε_{ax}) vs. time is shown for two oscillations. In addition the approximation function for ε_{ax} is depicted. At closer examination it is obvious that for specimens from CCTs the reaction in terms of deformation does not follow a simple sinusoidal function with linear term.

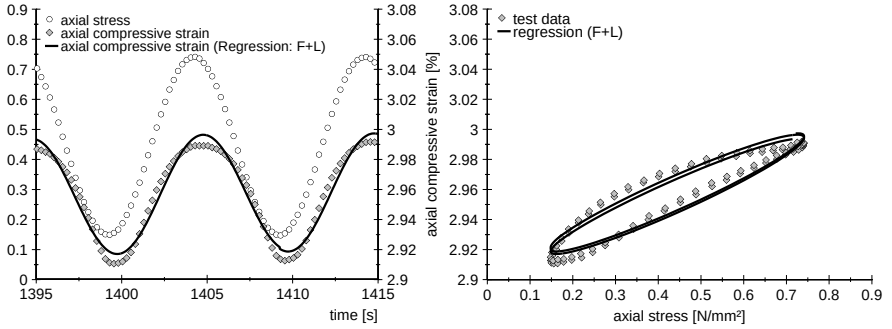

Fig. 4 Example of CCT test data with axial stress (σ_{ax}) and strain (ε_{ax}) and the analytical approximation *F+L* (a) in time domain; (b) as a stress-strain relationship

At the point of maximum loading the test data of deformation is broader and flatter whereas on the point of minimum loading the deformation appears narrower with a larger peak. The diagram on the right shows the stress-strain relationship for the same oscillations. It reveals more clearly that the test data differs from the *F+L* regression or rather that the function is not able to fit the test data with satisfactory quality. Especially in the loading and unloading phase, the shape of the test data shows a distortion compared to the sine approximation. For these reasons Kappl (2007) [7] introduced an advanced approximation function for the regression of CCTs, the *F+L+1H* regression. A second sinusoidal term was added representing the first harmonic of the oscillation characterized by the double frequency of the fundamental oscillation. **Fehler! Verweisquelle konnte nicht gefunden werden.** presents the same data as Fig. 4 but with the *F+L+1H* approximation. By comparing the Fig.s it becomes clear, that the advanced approximation fits the deformation data in a better way than the standard sine approach. This is true for the extrema as well as the loading and unloading phase. The F+L+1H approach accounts for distorted sinusoidal oscillations.

The advanced approximation function was used in [7] to describe the magnitude and shape of a distorted sine. The ratio of the amplitude of the 1st harmonic to the fundamental oscillation as well as the shift factor between the 1st harmonic and the fundamental influence affect the shape of the regressed function in terms of incline between the extremal values and the shape of the extrema respectively, as well as values of the extrema. The amplitude ratio is referred to as

$$AR = \frac{a_5}{a_2} \qquad (3)$$

where:

AR..... Ratio of amplitude of 1st harmonic to fundamental oscillation [-]

and the shift factor between both sinusoidal terms

$$\gamma = a_6 - a_3 \qquad (4)$$

where:

γ..... Shift factor between 1st harmonic and fundamental oscillation [°].

To systematically study the impact of the 1st harmonic a theoretic example with the following input parameters is given. The offset (a_1), the phase lag of the fundamental oscillation (a_3) as well as the linear term (a_4) are set to 0. The amplitude of the fundamental oscillation (a_2) is 1, the amplitude of the 1st harmonic (a_5) is set to 0.2. Since a_1 is 1, a_5 is equal to the amplitude ratio *AR* according to equation (3). The phase lag of the 1st harmonic (a_6) varies within a range of −180° to 180° to show the impact of this parameter. This particular range was chosen because the test results are usually within this area. Since a_3 is 0, a_6 is equal to the shift factor between both sinusoidal terms γ according to equation (4). The frequency *f* is set to 0.1 Hz. The parameter set is also shown in Table 5.

Table 5 Input data used for analysis of the advanced approximation function *F+L+1H*

Parameter	Values	Details
a_1	0	Offset
a_2	1	Amplitude of fundamental oscillation
a_3	0	Phase lag of fundamental oscillation
a_4	0	Gradient of linear term
a_5 = AR	0.2	Amplitude of 1st harmonic
$a_6 = \gamma$	−180° to 180°	Phase lag of 1st harmonic
f	0.1 Hz	Frequency

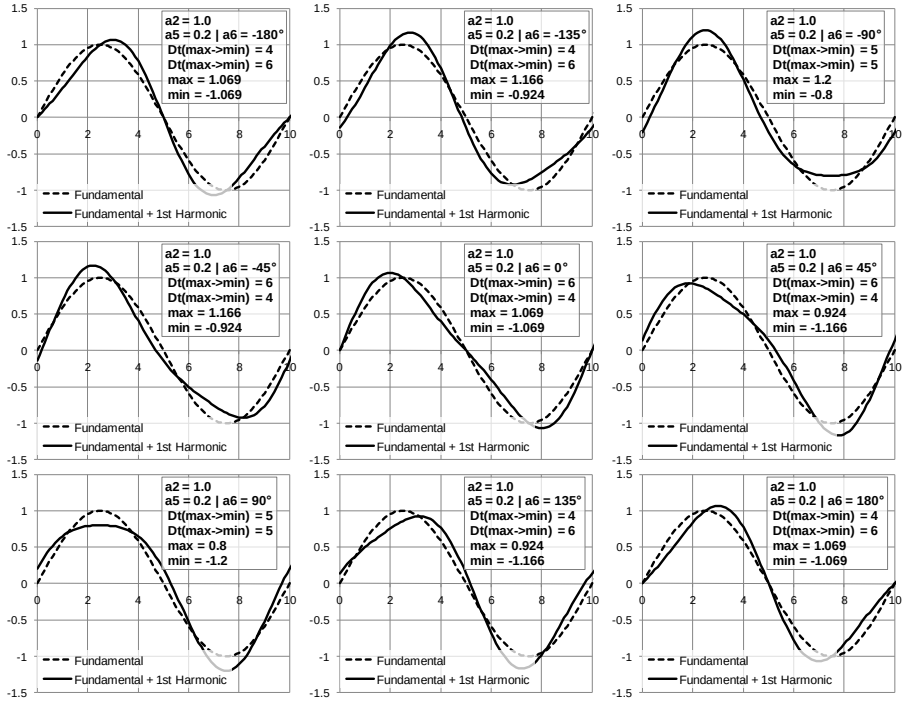

Fig. 5 Variation of shift factor between 1st harmonic and fundamental from a_6 = −180° (upper left) to +180° (lower right).

Fig. 5 shows nine diagrams with a systematical variation of the shift factor γ between fundamental and 1st harmonic. Starting from the top left at −180° γ is raised by +45° in each diagram to +180° at the bottom right. The following statements regarding the change of the function are made in comparison to the standard sinusoidal oscillation which is also shown in the diagrams.

At a shift factor of −180° the 1st harmonic's influence is dominant in the loading and unloading phase leaving the shape of the extrema unaffected. From −180° to −90° the impact of the 1st harmonic shifts to the other extreme. At −90° the shape around the extrema are clearly deformed. In terms of shape of the function the changing influence of the 1st harmonic on the deformation of the sine continues with a turning point every 90°.

What becomes clear is that the advanced function can be used to check the shape of a sine quickly by using *AR* and γ. The value of *AR* reflects the magnitude of the distortion (quantity of distortion), the shift factor γ describes in which way the sine is distorted (quality of distortion).

4. Results and Discussion

To investigate the impact of the connection between load plate and specimen on the material response, results from both test setups are compared in the following. Regression analysis of the test data was carried out with the *F+L* and the *F+L+1H* function. The diagrams in this section present the results as follows: The solid lines represent data from the unglued setup, the dashed line from the glued setup. The bold lines show the median values. The median values were derived from data of the four specimens tested in each setup at each test frequency. The thin lines around the median values represent the 95% confidence interval of the results.

The investigation starts with an analysis of signal data from the force sensor. Since the tests were carried out in a force-controlled way, this part of the study gives information about the quality of the control unit of the test machine, i.e. how good the quality of the sine produced by the test machine is. The next analysis deals with data from the axial deformation sensor. It is interesting to see to which extent the material response resembles a sine when the loading is sinusoidal in the compressive domain and whether there are differences between glued and unglued setup. The investigation is finalized by looking at the derived material response (stiffness and phase lag) in the linear viscoelastic domain from both setups and comparing the results of the CCTs to those from 4PBB stiffness tests.

4.1. Analysis of Signal Data from Force Sensor

This part of the study takes a detailed look on the data derived from the force sensor for the unglued and glued test setup. The left diagram in Fig. 6 provides a comparison of the coefficients of determination for the regression of the force sensor with the standard *F+L* function for both setups with respect to the test frequency. It is obvious that the fit quality is practically identical for both setups, and that the quality of the regression is at a very high level above 0.999. The coefficients of determination indicate that the test machine works with high quality in the tested range up to 10 Hz and there seems to be no difference between the two test setups.

The right diagram in Fig. 6 gives the analogue information for the advanced *F+L+1H* approximation. Again both setups are shown in the diagram. The situation is similar to the quality of fit for the standard approximation. Again, both setups result in similar and high fit qualities.

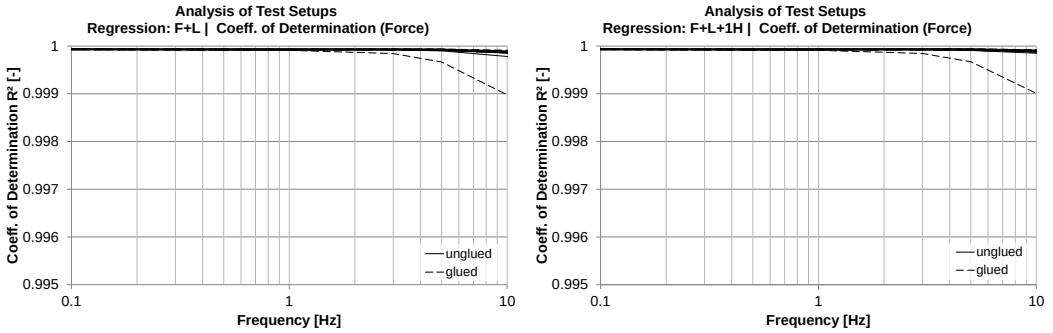

Fig. 6 Median value and 95% confidence interval of the coefficient of determination R^2 for the force sensor for glued and unglued test setup (a) F+L approximation; (b) F+L+1H approximation

The amplitude ration *AR* between 1st harmonic and fundamental oscillation of the approximation together with the shift factor γ is used to find out whether the shape of the sinusoidal force changes at different frequencies or between the two test setups. It gives more information than the coefficient of determination, since the two parameters describe quantity and quality of the distortion.

Fig. 7 presents the results. By taking a look at the amplitude ratio in the left diagram it becomes clear that there is no distinguishable distortion since *AR* is below 1‰ for lower test frequencies. *AR* increases with increasing frequency but still stays at very low level. Even at 10 Hz the median *AR* is only around 5‰. Thus, the test machine provides sinusoidal loading with hardly any distortion. But there is a clear, increasing trend of *AR* with increasing frequency indicating that the ability of the control unit to provide sinusoidal loading decreases. The 95% confidence interval of *AR* shows that there is no significant difference between both setups, although the median value of *AR* of the unglued setup is 20% higher than *AR* of the glued setup.

Data of the shift factor are presented in the right diagram. Again both setups produce the same γ. The scatter is rather large when testing at low frequencies. Due to the small *AR* this has no impact on the shape of the force approximation. The phase lag at 10 Hz is around -100°. Still, *AR* is so small that this has no noteworthy effect on the shape of the sinusoidal force.

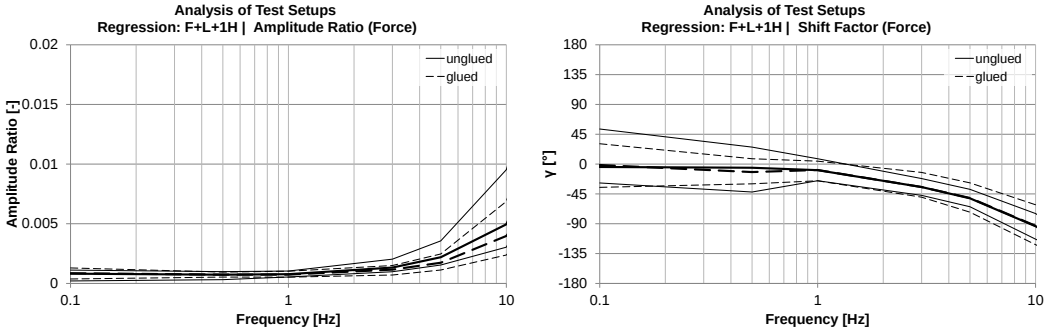

Fig. 7 Median value and 95% confidence interval of (a) AR; (b) γ - for the force sensor for glued and unglued test setup at 30°C.

This section proves that the test machine provides a sinusoidal loading with good quality in terms of shape of the oscillation. Also, the test setup, i.e. whether the specimen is glued to the load plates or not, has no relevant impact on the shape of the sinusoidal force signal.

4.2. Analysis of Signal Data from Deformation Sensor

Fig. 8 presents the coefficient of determination for the axial deformation sensor of both setups. The left diagram gives information about the regression with the standard approximation *F+L*. Clearly, both setups are fitted with a high quality (R^2>0.995) for the complete range of test frequencies. Scatter for both cases is similar.

The data show that the standard sine approximates the deformation data better at higher frequency. From 3 Hz on, the coefficient of determination R^2 is around or above 0.998. At low frequencies when the viscous part of the material behavior is still dominant, the standard approximation function describes the material behavior only at a lower, although good quality level.

The right diagram in Fig. 8 shows the results for the coefficient of determination R^2 for both setups with the advanced *F+L+1H* approach. Compared to the standard regression the quality of fit of both cases is considerably higher. For the unglued specimens the quality of fit R^2 is above 0.999 for the complete range of test frequencies with a low scattering. Especially at low frequencies where the viscous part of the material behavior is more dominant, the difference to the standard approximation is clear.

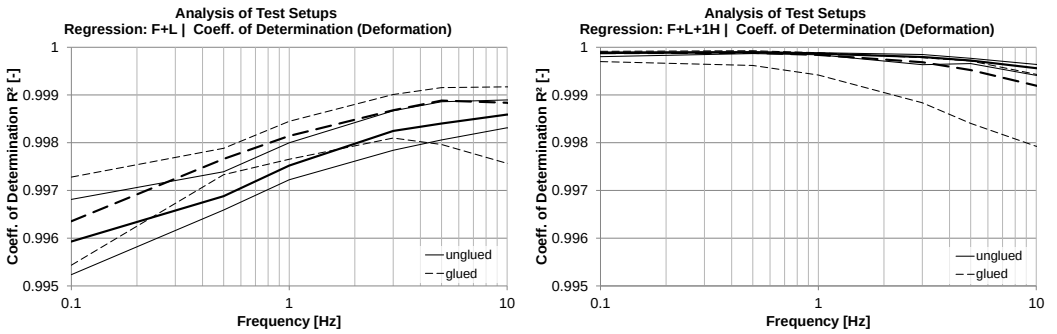

Fig. 8 Median value and 95% confidence interval of the coefficient of determination R^2 for the deformation sensor for glued and unglued test setup at 30°C- (a) F+L approximation; (b) F+L+1H approximation

Fig. 9 presents the amplitude ratio *AR* and the shift factor γ for the axial deformation data. There is a clear relation between *AR* and the test frequency. The higher the frequency and thus the more dominant the elastic part of the behavior gets, the lower becomes the share of the 1st harmonic term. Data from tests with both setups start around the same values at 0.1 Hz, the unglued setup at a range of 6.2% to 7.1%, and the glued setup ranges from 5.5% to 7%. The ratio decreases more quickly with increasing frequency for the glued setup reaching 1.4% to 2.4% at 10 Hz. The unglued setup results in a ratio of 2.4% to 3.6% at this frequency. In terms of the median values the unglued setup shows a 7% higher amplitude ratio at 0.1 Hz, increasing to a 42% higher ratio at 10 Hz compared to the glued setup. It can be stated that the impact of the 1st harmonic declines with increasing test frequency. This goes along with the data presented in Fig. 8 where the coefficient of determination was shown for the standard approximation function. The quality of fit of the standard function increases with increasing frequency. This is a logic result as the share of the 1st harmonic gets less dominant at these test conditions. For the whole frequency range, the ratio is smaller for the glued setup, showing that the deformation produced by the glued specimens is more related to a sinusoidal shape than for the unglued specimens.

The right diagram in Fig. 9 presents results of the shift factor γ. This value starts at -17° for the unglued and -19° for the glued setup (median values) at 0.1 Hz. This shows that there is a steeper incline of the approximation function in the loading and a flatter decline in the unloading phase. Up to 5 Hz, the shift factor stays beyond -45°. Simultaneously, *AR* decreases indicating that the difference in the gradient between loading and unloading phase gets smaller. When the test frequency is increased to 10 Hz, γ becomes even larger

reaching -60° for the glued and -50° for the unglued setup respectively. Together with a still decreasing amplitude ratio, the distortion of the deformation oscillation becomes less dominant.

It was shown in this section that the shape of the deformation cannot be described as well with the standard *F+L* regression as with the advanced *F+L+1H* function. This is especially true for low frequencies below 3 Hz. Glued specimens produce slightly better qualities of the fit with the standard approximation function. It is therefore assumed that glued specimens react with a less distorted sine to sinusoidal load in terms of deformation. This thesis is confirmed by the amplitude ratio between 1st harmonic and fundamental. It is also higher for the glued setup throughout the frequencies.

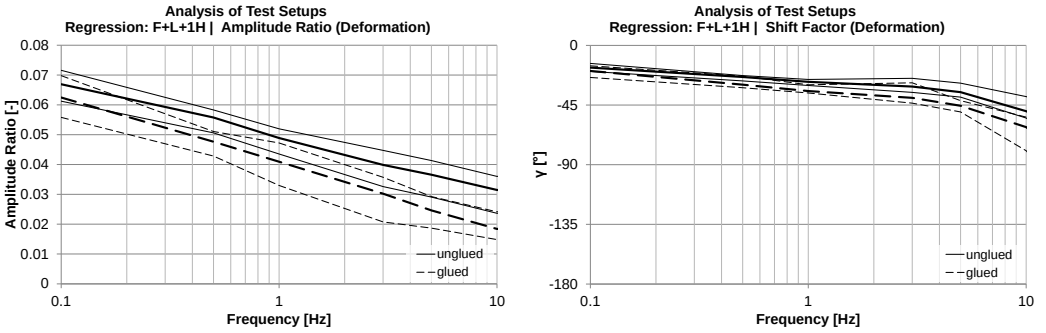

Fig. 9 Median value and 95% confidence interval of (a) AR; (b) γ - for the deformation sensor for glued and unglued test setup, as well as for 4PBB tests at 30°C

4.3. Analysis of Material Reaction in the Linear Viscoelastic Domain

So far the analysis was carried out for data from the force and deformation sensor. An interesting question is, if and how the test setup influences the derived material parameters. It is also important to analyze whether the derived material response from CCTs in the linear viscoelastic domain is comparable to results obtained from well-established stiffness test. Thus, 4PBB stiffness tests according to [9] were carried out on four specimens produced from the same mix. Results from 4PBB are shown in the diagrams of this section as dash-dotted lines. Again bold lines represent the median values from results of four specimens for each frequency. The thin lines around the median values represent the 95% confidence interval of the results.

In Fig. 10 the left diagram shows the axial phase lag ($\varphi_{ax,ax}$) between force and axial deformation when the regression is carried out with the *F+L* function for the CCTs. In addition it shows the phase lag φ derived from the 4PBB. The difference between the two analyzed CCT setups in terms of the axial phase lag is not significant. The median values of the phase lag show a difference below 1° for all frequencies. The largest difference between CCTs and 4PBB in terms of the phase lag can be found at 0.1 Hz, when the glued setup is considered. The median values have a difference of 2.2°. Still, the 95% confidence interval of both tests overlap even at 0.1 Hz. Thus, the difference can be seen as insignificant.

The right diagram in Fig. 10 shows results of the norm of the complex modulus $|E^*|$ for both CCT setups and the 4PBB. Before looking at the data, it must be noted the volumetric characteristics of the specimens differ considerably. When the data about the air void content of the tested specimen is taken into consideration (see Table 2 and Table 4) it can be seen that mean value of the void content of the specimens tested in the unglued setup is 6.0% (v/v), whereas it is 4.0% (v/v) for specimens tested in the glued setup. For specimens tested in the 4PBB the mean value of the air void content is 4.2% (v/v) and is thus comparable to the specimens used for glued tests. It was shown by Hofko and Blab (2012) [12] that the air void content has a significant impact on the

material stiffness in terms of norm of the complex modulus. This effect was found to be 4 times more severe for high frequencies (10 Hz) than for low frequencies (0.1 Hz). The same ratio can be found for the norm of the complex modulus of the CCTs presented in this paper. The difference between unglued (higher void content) and glued (lower void content) setup is 130 MPa at 0.1 Hz and 540 MPa at 10 Hz. Thus, it is concluded from the findings of this research and the study [12] that the difference in modulus between both setups is related to the different volumetric characteristics of the specimens and not to the difference in test setup. When data from the 4PBB specimens are considered as well, it can be noted that the difference between results from glued tests and 4PBB (comparable void content) is moderate with the largest difference occurring at 1 Hz with 162 MPa or 10.4%. When the 95% confidence interval is considered, the difference between both test types is not significant. It can be concluded that the material response in terms of stiffness and phase lag within the linear viscoelastic domain obtained from CCTs is comparable to well-established and standardized stiffness tests like the 4PBB.

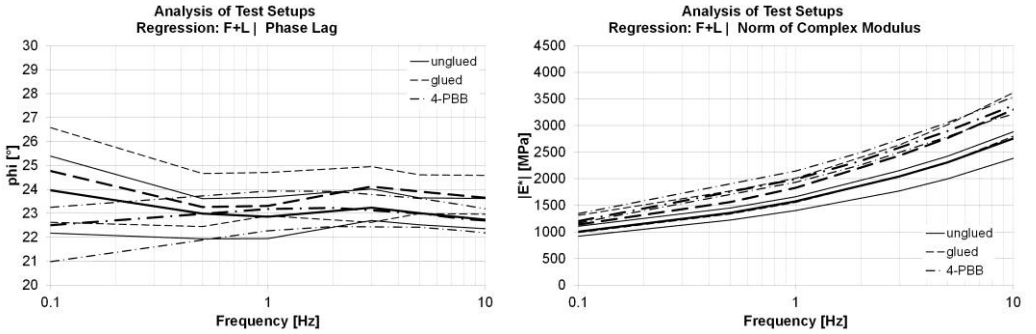

Fig. 10 Median value and 95% confidence interval of (a) $\varphi_{ax,ax}$; (b) |E*| - for glued and unglued test setup, as well as for 4PBB tests at 30°C, F+L approximation

5. Conclusions

From the analysis of two different CCT setups with an advanced *F+L+1H* regression, and the comparison of results with 4PBB tests, the following conclusions can be drawn:

- The advanced *F+L+1H* approximation function is a proper tool to quickly check the shape of sinusoidal functions. If the sine is distorted, the amplitude ratio *AR* and the shift factor γ are able to describe the magnitude and shape of the distortion.
  The *F+L+1H* approach can give valuable information about the shape of oscillating test data. Problems with the test machine control as well as shape and magnitude of the deformation oscillation can be detected and described easily.
- Regarding the data of the force sensor, no significant distortion of the sinusoidal loading can be found. Both setups result in a high quality of fit with the standard and the advanced regression approach for the complete frequency range. The amplitude ratio *AR* is very low (<5‰) for frequencies up to 10 Hz. Thus, there is no noteworthy distortion of the sinusoidal force. Since the tests were carried out in a force-controlled way, the results indicate that the control unit of the test machine works with high quality at least up to 10 Hz regardless of the connection between specimen and load plate.
- The analysis of data of the deformation sensor revealed that the deformation cannot be approximated as well with the standard sinus as the force data. The fit quality of the glued setup is better when the *F+L* function is used for regression analysis. The advanced approach results in coefficients of determination of 0.999 and higher for both setups. By considering the amplitude ratio *AR* it was found that especially at lower frequencies (with a more dominant viscous material behavior) the shape of the deformation is distorted with a steeper

incline of the loading phase and a flatter decline in the unloading phase. The effect is stronger for unglued specimens.

- In terms of mechanical material parameters it was found that there is no difference in phase lags between both setups. There is also no significant difference between phase lags from 4PBB tests and the CCTs.
- When it comes to material stiffness in terms of norm of complex modulus, unglued specimens reacted less stiff than glued specimens. It could be shown that this effect is connected to the different content of air voids of the tested specimens and not to the difference in test setup. Again, no significant differences between results from 4PBB tests and the CCTs occurred.
- Thus, it can be concluded that tests in the compressive domain are capable of describing the material parameters of HMA in the linear viscoelastic domain regardless of the connection between load plates and specimen and that the results derived from CCTs are comparable to those derived from 4PBB.

References

[1] Francken L (1977) Permanent deformation law of bituminous road mixes in repeated triaxial compression. Proceedings of the 4th international conference on structural design of asphalt pavements, Ann Arbor
[2] European Standard EN 12697-25(2005) Bituminous mixtures - Test methods for hot mix asphalt - Part 25: Cyclic compression test
[3] Jaeger W (1980) Mechanical Behavior of Hot Mix Asphalt Specimens (Mechanisches Verhalten von Asphaltprobekörpern). Publication of the Institute of Road and Railway Engineering, University of Karlsruhe, Germany
[4]Weiland N (1986) Deformation Behavior of Hot Mix Asphalt Specimens under repeated loading (Verformungsverhalten von Asphaltprobekörpern unter dynamischer Belastung. Publication of the Institute of Road and Railway Engineering, University of Karlsruhe, Germany
[5] von der Decken S (1997) Triaxial tests with sinusoidal axial and radial loading to investigate the deformation resistance of hot mix asphalt (Triaxialversuch mit schwellendem Axial- und Radialdruck zur Untersuchung des Verformungswiderstandes von Asphalten). Publication of the Institue of Road Engineering, Technical University of Brunswick, Germany
[6] Kappl K (2007) Assessment and modeling of permanent deformation behavior of bituminous mixtures with triaxial cyclic compression tests. Dissertation, Vienna University of Technology, Austria
[7] Hofko B (2011) Towards an enhanced characterization of the behavior of hot mix asphalt under cyclic dynamic compressive loading. Dissertation, Vienna University of Technology, Austria, http://www.ub.tuwien.ac.at/diss/AC07812414.pdf
[8] Di Benedetto H, Partl M, Francken L, De La Roche Saint André C (2001) Stiffness testing for bituminous mixtures. Materials and Structures, 34, 2, p 66-70, Springer Netherlands, 66-70, Doi: 10.1007/BF02481553
[9] European Standard EN 12697-26 (2004) Bituminous mixtures - Test methods for hot mix asphalt - Part 26: Stiffness
[10] Hoeflinger G (2006) Investigation of specimen preparation of hot mix asphalt using the segment roller compactor. Master Thesis, Vienna University of Technology, Austria
[11] Airey G, Rahimzadeh B and Collop A (2003) Viscoelastic Linearity Limits for Bituminous Materials. Proceedings of the 6th International RILEM Symposium on Performance Testing and Evaluation of Bituminous Materials, Zurich, Switzerland
[12] Hofko B and Blab R (2012) Impact of air void content on the viscoelastic behavior of hot mix asphalt. Proceedings of the 3rd Four-point bending beam conference, Davis, CA.